GEOMETRIC POTENTIAL
An Explanation of Nanofiber's Wettability

by

Peng LIU[a] and Ji-Huan HE[a,*]

[a] National Engineering Laboratory for Modern Silk, College of Textile and Clothing Engineering, Soochow University, Suzhou, China

Original scientific paper
https://doi.org/10.2298/TSCI160706146L

Similar to Casimir force, nanofibers have a potential that attracts water molecules, while the porosity of the nanofiber mat produces a repelling force. Wetting property of a nanofiber mat is a result of combination of the forces and gravity. A new concept, the geometric potential or the boundary-induced force, is introduced to elucidate the basic property of wetting. Various nanofiber mats with different fiber morphologies are fabricated by the bubble electrospinning. The paper concludes that superhydrophobic properties of nanofiber mat depends upon mainly fiber morphology and porous structure of the mat, hydrophilic properties of ZnO nanorods will not affect the water contact angle much.

Key word: *Casimir force , nanofibers, ZnO nanorods, wetting properties*

Introduction

Why does some fabric behave superhydrophobically like a lotus leaf? Why does other fabrics are superhydrophilic like a capillary? There must be a force on the surface of fabrics that either attracts or repels water molecules. The morphology of the fabric surface plays an important role in this surface property.

All forces are due to boundary interaction of two bodies, one is the acting body, *e. g.*, the Sun, and the other is the acted body, *e. g.*, the Earth, conversely a boundary is formed due to interaction of two or multiple forces, for example a dune is a result of blowing air and friction [1].

Most energy is hidden on the boundary, a good explanation of this phenomenon is the well-known stress concentration, which always arises in sharp change of surface. We call the boundary energy as geometrical potential [1-3]. Another example is the capillary phenomenon, see fig.1, the boundary-induced force or the geometrical potential in capillaries is powerful enough to pull water upward step by step to a height of 90 meters in a tree, it requires 8.7 atm to pump water to such a height.

For a spherical boundary, the boundary-induced force can be expressed as [1]:

$$F = \frac{\partial E}{\partial R} \propto \frac{1}{R} \tag{1}$$

For a smooth boundary, eq. (1) can be written in the form [1]:

* Corresponding author, e-mail: hejihuan@suda.edu.cn

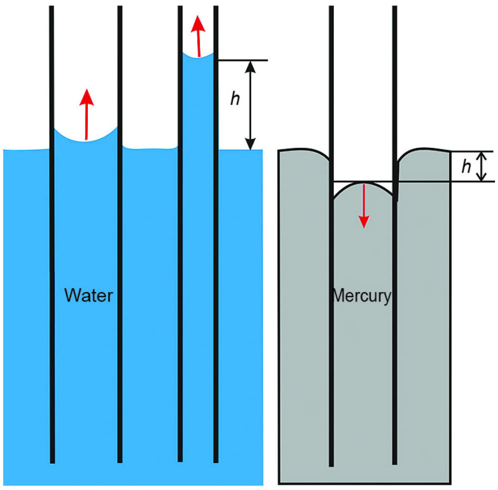

Figure 1. Capillary

$$\vec{F} \propto \nabla f \tag{2}$$

where R is the curvature radius of the surface, $f(x, y, z) = 0$ – the surface equation, E – the geometrical potential. When R tends to zero, the force becomes infinitely large, this is generally considered as stress concentration in mechanical engineering.

A boundary-induced force arises when a surface is curved, that might be gravitational force in celestial bodies; gravitation of all matters on the Earth's surface; atom-scale force on the curved 2-D world sheet of string. We consider a capillary as illustrated in fig. 1. Balance of the boundary-induced force (capillary force) with gravity requires that:

$$k\frac{1}{R} = \rho g h \tag{3}$$

where k is a constant, ρ – the density, g – the gravitational acceleration, and h – the height of a liquid column. According to the capillary theory, the height h of a liquid column is given by:

$$h = \frac{2\sigma \cos\theta}{\rho g R} \tag{4}$$

where σ is the liquid-air surface tension (force/unit length), and θ – the contact angle. We can see that both eq. (3) and eq. (4) predicts $h \propto 1/R$.

To elucidate the reliability of our analysis, we consider the gravity on the Earth's surface, which is caused by the curved space (the spherical Earth) and its density, the gravity acceleration can be expressed in a scale form [4]

$$\vec{g} \propto \rho \nabla f \tag{5}$$

where f is the Earth's surface, $f(x, y, z) = x^2 + y^2 + z^2 - r^2 = 0$, r – the average radius of the Earth, $\rho = M/(4/3\ \pi r^3)$, and M – the Earth's mass. The boundary-induced force scales:

$$\nabla f(x, y, z) = 2x\vec{i} + 2y\vec{j} + 2z\vec{k} = 2\vec{r} \tag{6}$$

We, therefore, obtain:

$$g \propto \rho r \propto \frac{M}{r^2} \tag{7}$$

This agrees exactly with that obtained by Newton's gravitational law [4].

The motion of a tectonic plate will greatly affect local gravity due to its change of the geometrical potential. Similarly change of lithosphere will produce boundary-induced force, that will affect gravity, and create an anti-gravity illusion that water moves suddenly upwards or volcano occurs, see fig. 2, such anti-gravity phenomena also occurs before the earthquake.

Experiment design

This paper will design an experiment to verify our theory by studying the wetting property of nanofibers with different morphologies. In this experiment, aligned PVDF/Fe_2O_3/Zn(Ac)$_2$ nanofiber mats were fabricated using bubble electrospinning [5, 6] with a magnetic field, fig. 3(a). A direct current (DC) voltage of 15 kV was applied between the nozzle and grounded aluminum foil collector with a distance of 12 cm. The length of the gap between the two parallel-positioned permanent magnets is 4 cm. Subsequently, the as-spun nanofiber mats were thermally treated in air at 140 °C for 24 hours to obtain ZnO nanoparticles. ZnO nanorods grown on nanofibers can be obtained by the hydrothermal method [7-9]. Figure 3 illustrates the fabrication process of the aligned ZnO nanorods on surface of PVDF/Fe_2O_3/Zn(Ac)$_2$ composite nanofiber membranes.

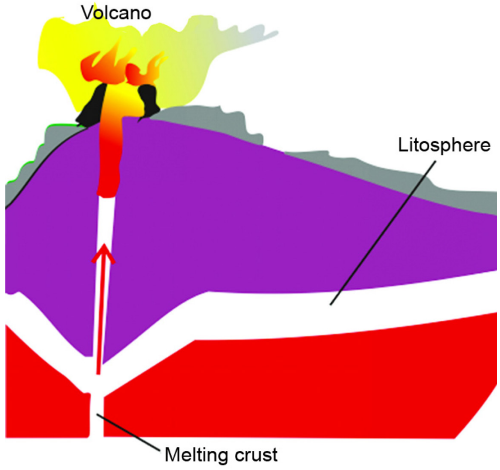

Figure 2. Volcanic eruption due to an upward boundary-induced force

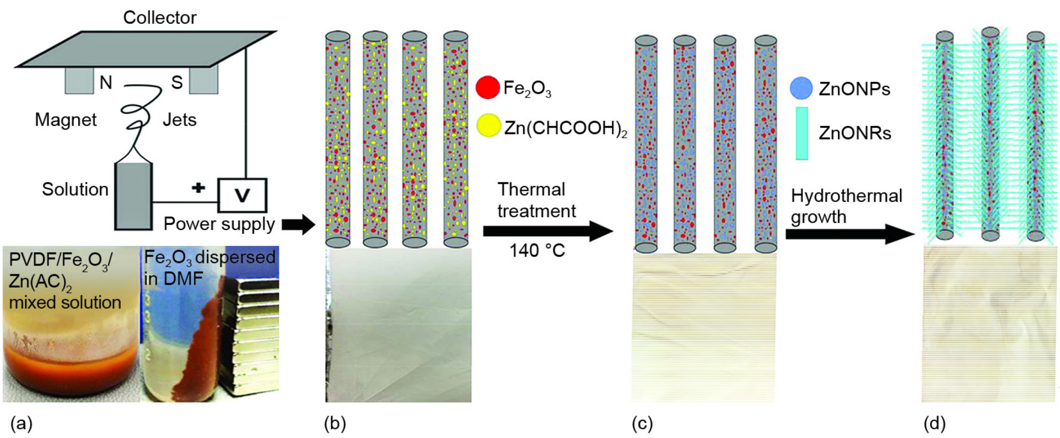

Figure 3. Schematic illustration for the preparation process of hierarchical aligned ZnO nanorods on surface of PVDF/Fe_2O_3/Zn(Ac)$_2$ composite nanofiber membranes

Figure 4 shows the SEM illustrations for our four samples. Sample a, fig. 4(a) is obtained by the bubble electrospinning without adding magnetic field. Sample b, fig. 4(b) is the aligned PVDF/Fe_2O_3/Zn(Ac)$_2$ nanofibers, which were successfully fabricated using electrospinning with a magnetic field [7, 8]. Water contact angle (WCA) was measured for each sample to examine the surface wettability and adhesion of water on the nanofibers membrane, see fig. 5.

Figure 4(b) displays the SEM images of the aligned PVDF/Fe_2O_3/Zn(Ac)$_2$ nanofibers, which were successfully fabricated using bubble electrospinning with a magnetic field.

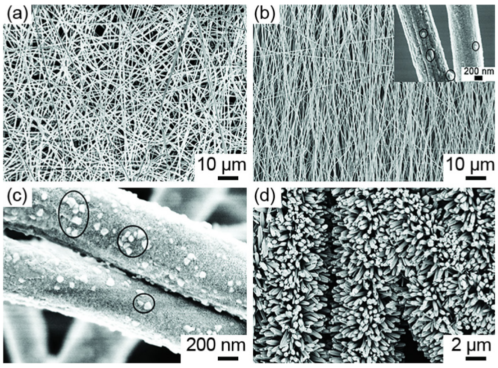

Figure 4. The SEM images of $PVDF/Fe_2O_3/Zn(Ac)_2$ nanofibers; (a) misaligned nanofibers, (b) aligned nanofibers, (c) aligned nanofibers without hydrothermal treatment, (d) aligned nanofibers after hydrothermal treatment

On the contrary, fig. 4(a) shows a typical misaligned $PVDF/Fe_2O_3/Zn(Ac)_2$ nanofiber mats *via* bubble electrospinning without adding magnetic field. A possible reason for formation mechanism of aligned fibers is that magnetic nanoparticles tend to form lines due to the magnetic force of parallel magnetic field [10, 11]. Therefore, the magnetic field plays a significant role in the process of spinning, which is responsible for the alignment of the magnetic nanoparticle (Fe_2O_3) doped fibers. In spite of this, all of these randomly oriented and orderly oriented $PVDF/Fe_2O_3/$ $/Zn(Ac)_2$ nanofibers have a uniform morphology with a similarly average fiber diameter.

As can be clearly seen, unheated as-spun nanofibers, fig. 4(b) with a few number of the heterogeneous distribution nanoparticles, the possible reason is due to the present of Fe_2O_3 NP and it can not completely effectively dispersed into the solution. However, it is clearly observed that amounts of nanoparticles are spread all over the surface of the heated as-spun nanofibers from fig. 4(c). This can be explained due to the decomposition or transformation of zinc acetate.

Figure 4(d) shows SEM images of ZnO nanorods grown around the heated as-spun nanofibers after hydrothermal process. It was evident to us that a very uniform coverage ZnO nanorods arrays grew onto the entire length of the heated as-spun nanofibers, which contribute the growth-induced seeds layer in the fibers surface. These results have confirmed that heat treatment has made the parts of zinc acetate into zinc oxide. All of the ZnO nanorods have a hexagonal cross-section with a diameter in the average about 240 nm.

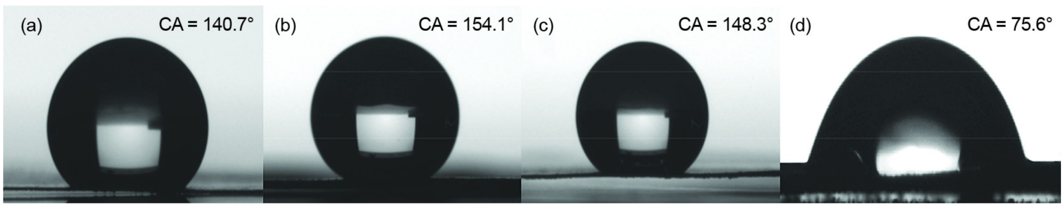

Figure 5. The CA of as-spun mats; (a) unheated and misaligned, (b) unheated and aligned, (c) heated and aligned without hydrothermal treatment, (d) heated and aligned after hydrothermal treatment

Theoretical analysis

We consider a section of nanofiber mat, between two adjacent fibers, there is a space, see fig. 6. When a water molecule is approaching to the fibers' surface, Casimir-like force arises [12]. The adjacent nanofibers have geometrical potential to attract water molecules, while the space between the two adjacent nanofibers, which has an opposite curvature, can repel the water molecules. The balance of gravity, attracting force and repelling force results a water bridge between the two fibers.

Figure 5(a) shows the WCA of misaligned PVDF/Fe_2O_3/Zn$(Ac)_2$ nanofiber mats is 140.7°. The aligned nanofiber mat shows superhydrophobic properties with WCA of 154.1° in fig. 5(b). The aligned nanofiber mat has regular space between fibers as illustrated in fig. 7, while the misaligned nanofiber mat does not have such a property, random space is predicted. A longer distance of the adjacent fibers predicts a weaker repelling force, see fig. 1, as a result, its water contact angle becomes smaller.

Now we study the effect of ZnO nanorods on the water contact angle. The ZnO is considered to be hydrophilic. This is due to the weak charge interaction as illustrated in fig. 8. That means that some water molecules will be attracted into the surface of ZnO nanorods, this affects water contact angle. Figure 4(c) shows some ZnO nanoparticles on fiber's surface, and its water contact angle does not change much compared with that for sample c. However, when the ZnO nanorods are grown on the surface of the fiber, as illustrated in fig. 4(d), the interaction between water and ZnO weakens the water bridge between two adjacent fibers, as a result, the water contact angle become smaller, fig. 9.

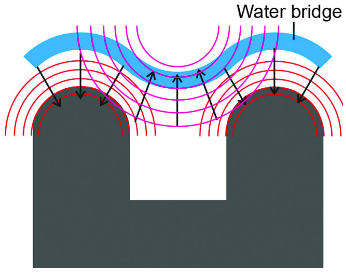

Figure 6. A water bridge due to gravity and geometrical potentials

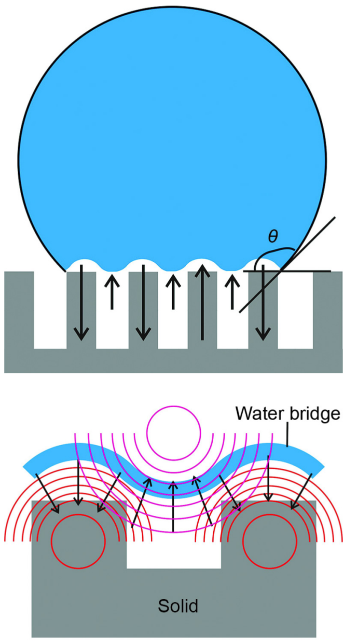

Figure 7. Differential geometrical potentials affect water contact angles

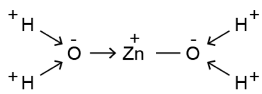

Figure 8. Weak charge interaction between water and ZnO

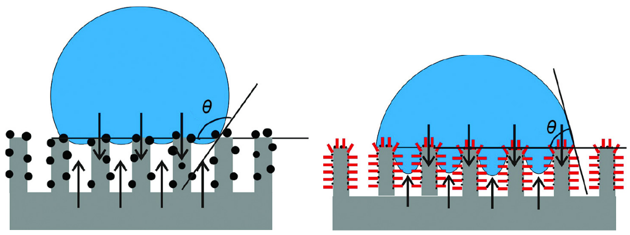

Figure 9. Effect of ZnO on water contact angle; right: ZnO nanoparticles on the fiber's surface, left: ZnO nanorodes on the fiber's surface

Conclusion

The wettability of materials is of much importance for various of specialty applications, which has attracted a great deal of concern. In general, water contact angle is one of the most commonly used method to characterize the wettability of a surface against liquid. This paper gives an explanation of wetting property through the geometric potential. Hydrophilic group and surface morphology are two main factors affecting the water contact angle.

Acknowledgment

The work is supported by Priority Academic Program Development of Jiangsu Higher Education Institutions (PAPD), National Natural Science Foundation of China under grant No. 11372205, Research and Innovation Project for College Graduates of Jiangsu Province under grant NO. SJZZ15_0162.

References

[1] He, J.-H., A Note on Elementary Cobordism and Negative Space, *International Journal of Nonlinear Sciences and Numerical Simulation, 11* (2010), 12, pp. 1093-1095
[2] He, J.-H., Frontier of Modern Textile Engineering and Short Remarks on Some Topics in Physics, *International Journal of Nonlinear Sciences and Numerical Simulation, 11* (2010), 7, pp. 555-563
[3] He, J.-H., Inverse Problems of Newton's Laws, *International Journal of Nonlinear Sciences and Numerical Simulation, 10* (2009), 9, pp. 1087-1091
[4] He, J.-H., An Elementary Introduction to Recently Developed Asymptotic Methods and Nano-mechanics in Textile Engineering, *International Journal of Modern Physics B, 22* (2008), 21, pp. 3487-3578
[5] Liu, P., *et al.*, Micro-Nanofibers with Hierarchical Structure by Bubbfil-Spinning, *Thermal Science, 19* (2015), 4, pp. 1455-1456
[6] Cui, Q. N., *et al.*, Effect of Temperature on the Morphology of Bubble-electrospun Nanofibers, *Thermal Science, 18* (2014), 5, pp. 1707-1709
[7] Athauda, T. J., *et al.*, One-Dimensional Hierarchical Composite Materials Based on ZnO Nano-Wires and Electrospun Blend Nanofibers, *RSC Advances, 3* (2013), 44, pp. 21431-21438
[8] Tolba, G., *et al.*, Hierarchical TiO_2/ZnO Nanostructure as Novel Non-Precious Electrocatalyst for Ethanol Electrooxidation, *Journal of Materials Science & Technology, 31* (2015), 1, pp. 97-105
[9] Han, J., *et al.*, Hydrothermal Growth of Mop-Brush-Shaped ZnO Rods on the Surface of Electro-Spun Nylon-6 Nanofibers, *Ceramics International, 39* (2013), 3, pp. 3095-3102
[10] Yang, D. Y., *et al.*, Fabrication of Aligned Fibrous Arrays by Magnetic Electrospinning, *Advanced Materials, 19* (2007), 21, pp. 3702-3706
[11] Liu Y. M., *et al.*, Magnetic-Field-Assisted Electrospinning Highly Aligned Composite Nanofibers Containing Well-Aligned Multiwalled Carbon Nanotubes, *Journal of Applied Polymer Science, 132* (2015), 22, pp. 41995
[12] Soroush, R., *et al.*, Modeling of the Casimir Force-Induced Adhesion in Freestanding Double-Sided Nanostructures Made of Nanotubes, *Nonlinear Science Letter A, 8* (2017), 2, pp. 149-155

Paper submitted: July 6, 2016
Paper revised: October 25, 2016
Paper accepted: December 25, 2016